Advanced Materials　～夢をかたちに～

新素材ニュース

CRDAM News letter

共同研究開発センター

Vol. 2
2013.11

CONTENTS

東北大学　金属材料研究所　附属新素材共同研究開発センター
Cooperative Research and Development Center for Advanced Materials,IMR,Tohoku University

活動報告

片平まつり２０１３「きんけん一般公開」に出展・展示

平成 25 年 10 月 12、13 日の二日間にわたって片平まつり 2013「きんけん一般公開」が開催されました。

この催しは、大学内 7 つの研究所等が行う一般公開行事で、今回で 8 回目の開催となります。

今回は「おっ！マテリアルっておもしろい？！」をキャッチフレーズに日頃の研究成果について教職員が分かりやすく説明をさせていただく他、来場者に楽しんでいただける参加型イベントで、当センターでは金属ガラス製のパターを用いてゴルフに挑戦していただき、ブースへの来場者 450 名程にエコカイロ等の景品を配布しました。

この催しの金研全体への来場者数は 4,000 人を越え、大変盛況でした。

（文責：横山　嘉彦）

活動報告

テネシー大学 Wojciech Dmowski先生（客員准教授）による講演会開催

平成 25 年 7 月 29 日（金）、国際教育研究棟セミナー室 2 において、新素材共同研究開発センター客員准教授 Wojciech Dmowski 先生（テネシー大学准教授）による講演会を開催しました。

先生は同大学およびホクリッジ国立科学研究所を兼務しておられる江上毅教授とシンクロトロンX線およびスパレーション中性子を用いた液体構造および金属ガラスの研究をされております。

今回は、"Atomic Structure and Mechanical Deformation in BMG"と題してご講演いただき、沢山の学生、研究者に聴講いただきました。

（文責：横山　嘉彦）

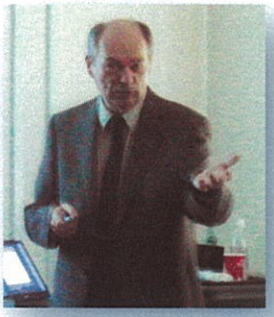

講演をする Dmowski 先生

セミナー" Research on Advanced Materials" 開催

Mattern 先生

平成 25 年 9 月 27 日（金）、国際教育研究棟セミナー室 2 において、韓国延世大学教授 Do Hyang Kim 先生、韓国清州大学教授 Won-Tae Kim 先生、ソウル国立大学准教授 Eun-Soo Park 先生、そして現在本学客員教授の Mattern Norbert 先生に、新素材研究における最近のトピックスについてご講演いただくセミナーを開催しました。

Park 先生

Mattern Norbert 先生には「Structure formation of two-phase glassy alloys」、Eun-Soo Park 先生には「Evaluation of glass-forming ability throught TTT diagram measured by electrostatic levitation」、Do-Hyang Kim 先生には「Application of Metallic Glass for High Performance Si Solar Cell-Oxidation Behaviour of Metallic Glass」、Won-Tae Kim 先生には「Phase-field simulation for multicomponent and multiphase alloy」と題しそれぞれご講演をいただきました。

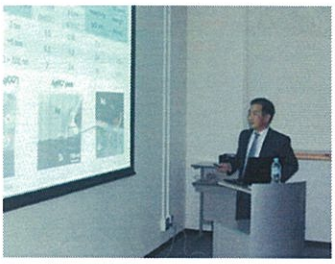

Do-Hyang Kim 先生

Won-Tae Kim 先生

（文責：横山　嘉彦）

就任挨拶

新素材共同研究開発センター　助教　　張　岩

１１月１日付にて新素材共同研究開発センターの教育研究支援者からこの度、助教として着任致しました。

私は平成 19 年から 5 年間、牧野研究室において学生として在籍し、鉄基アモルファス合金およびナノ結晶軟磁性磁心材料に関する研究を行ってきました。

鉄を主体とする軟磁性材料は発電、送電、配電、消費に重要な役割を果たしています。特に、最近の省エネルギー化の要求を背景に、自動車の低燃費化、各種電気機器の省エネ化、各種の産業機器あるいはエネルギー分野、インフラ設備等の幅広い領域において、それらに用いられているモータの高効率化が求められ、現在の主力材料である Fe-Si 合金に代わるより低磁気損失な軟磁性磁心材料の技術開発が必須課題として注目されています。ここで、磁気損失のうち、鉄損はヒステリシス損と渦電流損に分けられ、鉄損の減少は主に保磁力の低減（ヒステリシス損の減少）や電気抵抗率の増加（渦電流損の減少）などの方法を通じて実現できます。保磁力は磁心材料の原料純度、結晶磁気異方性、磁歪、欠陥や不純物や気孔などによる磁壁の移動に密接に関連しています。電気抵抗率は材料の内部微細構造と絶縁物被膜などに依存しています。しかし、保磁力の低減と電気抵抗率の増加は、磁化の低減をまねく場合があります。近年、電子・電気機器の高速化、高効率化の要求により、高周波への対応も求められています。高周波特性を有する従来材、例えばセンダストやソフトフェライトなどの材料は磁束密度が小さいために満足できません。つまり、将来の軟磁性材料の開発要点は高磁束密度と低磁心損失を併せもつ材料です。

私自身もとより微力ではございますが、これまでに学んだ軟磁性材料に関する専門知識、製造技術、分析手段などを充分に生かして、より一層、優れた研究成果を生み出すための効率的な研究に努め、新素材共同研究開発センターの発展のみならず金属材料研究所ならびに東北大学の材料科学分野の発展に深く寄与する優れた研究を目指す所存です。

どうかご指導の程よろしくお願い申し上げます。

H25 年度外国人客員研究員研究成果報告

Study of scintillation mechanism in $SrHfO_3$, $SrZrO_3$ and garnet-based ceramics

Prof. Martin NIKL

Department of Optical Materials, Institute of Physics, Academy of Sciences of the Czech republic, Cukrovarnicka 10, 162 53 Prague, Czech Republic

I was invited to work as a visiting professor at Advanced Research Center of Metallic Glasses in the Institute for Materials Research of Tohoku University from June 1 till July 31, 2013. During my stay I worked together with Professor Akira Yoshikawa and members of his laboratory. My group in the home institute in Prague has long (from 2002) and very successful collaboration with the group of Prof. A. Yoshikawa which has resulted in more than 130 publications so far. As the topic of my stay in IMR in 2013 we have selected the optical ceramics based on high density strontium hafnate as we have recently revealed that nonstochiometric material of the formula $Sr_iHf_{2-i}O_{4-I}$, i = 0.9 – 0.95 shows very intense radioluminescence in near UV, fig. 1, with reasonably fast decay time of about 180 ns at room temperature.

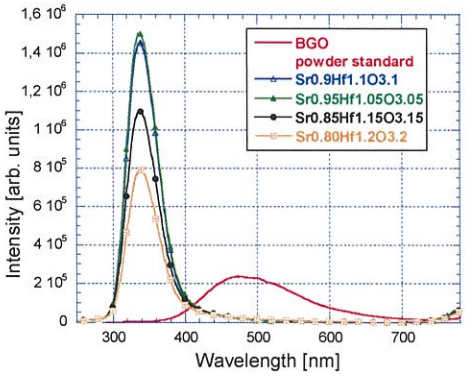

Fig. 1 Radioluminescence spectra of nonstochiometric SHO. X-ray excitation, 40 kV.

Starting powders for optical ceramics preparation were made in composition $Sr_{0.9}Hf_{1.1}O_{3.1}$ by a multi-step solid state sintering procedure with the annealing temperature within 1 100 – 1 200 ^{0}C. The grain size of the prepared powders was of the order of several microns, fig. 2

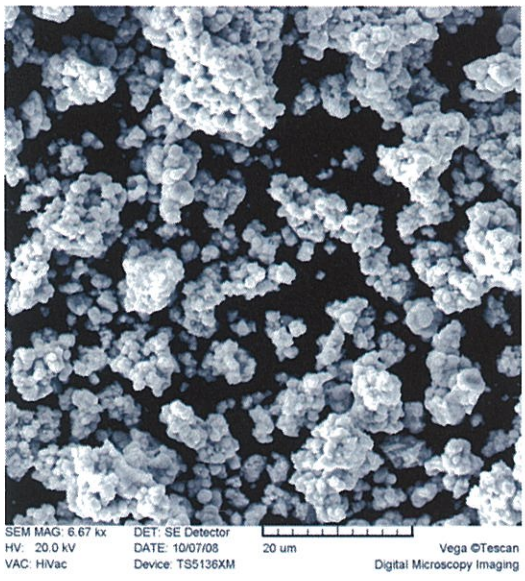

Fig. 2 SEM photo of the prepared SHO powder.

Their radioluminescence characteristics matched well those in fig. 1.

Spark plasma sintering (SPS) method was used in IMR to produce the ceramic material using the machine DR. SINTER (Fuji Denpa), fig. 3, the SPS condition were as follows: pressure: 100 MPa; temperature: X °C, 45 min, (x=1,600, 1,700, 1,800, 1,900) in vacuum (a few Pa). Prepared samples were of black appearance, fig. 4, due to strongly reductive conditions of the preparation procedure

Fig. 3 SPS apparatus DR.SINTER (Fuji Denpa) in Cooperative Research and Development Center for Advanced Materials / IMR.

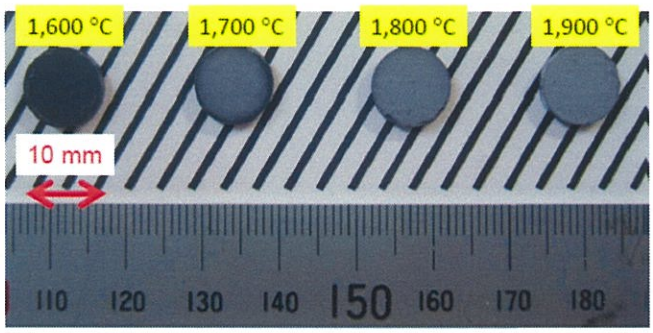

Fig. 4 SHO samples prepared by SPS method. Preparation temperature is noted above each sample.

Photoluminescence properties of ceramic samples were tested by Hamamatsu, C9920-02G spectrometer and the results are shown for two preparation temperatures in fig. 5. Under the excitation within 270 – 320 nm each sample shows two emission peaks at about 340 nm (identical with that of the starting powder) and 560 nm. The latter luminescence comes probably from lattice defects related to oxygen deficiency of ceramic. Well-resolved luminescence signal was observed for the samples prepared at temperatures T $\geq$1700 ^{0}C.
The samples will be further elaborated by annealing in air to restore the oxygen deficiency and carbon deposits and their luminescence will be continuously tested.

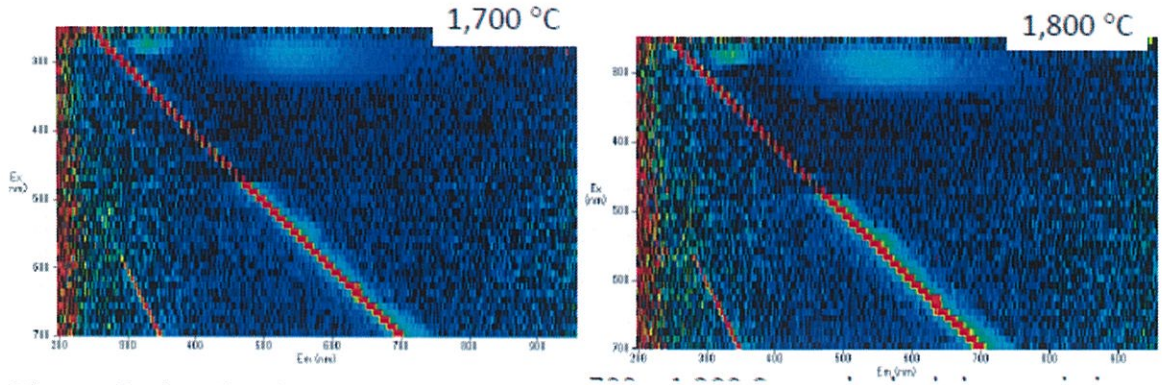

Fig. 5 2D photoluminescence spectra of ceramic samples from Fig. 4.

During my stay we have prepared with Prof. Yoshikawa the collaborative program and project proposal for next two years which will be submitted to JSPS and Czech Ministry of schools in the presently opened call. We have also agreed with Prof. T. Goto to write down a chapter reviewing the preparation of optical ceramics by SPS method for my book project approved in Pan Standford Publ. house.
I have also enjoyed very much meeting the other colleagues in IMR and discussing the forefront of the research related to optical and dielectric materials.

Acknowledgement
I would like to thank Prof. Makino, the Chair of Cooperative Research and Development Center for Advanced Materials in the Institute for Materials Research of Tohoku University, for giving me this fruitful opportunity to visit and continue our excellent collaboration with this institution.

Structure of $(ZrCu)_{90}Al_{10}$ Bulk Metallic Glasses

Prof. Wojciech Dmowski
Dept. of Mat. Sci. and Eng., University of Tennessee, Knoxville, TN 37996, USA.

Introduction

Metallic glasses (MGs) are structurally disordered metallic solids without translational symmetry and a well-defined unit cell. They are usually prepared by quenching alloys from the melt, bypassing crystallization. They may be considered to be a liquid frozen at the so-called glass transition temperature. The critical step in the development of glassy alloys happened in late 90's when Zr containing bulk metallic glasses (BMG) were discovered [1,2].The random atomic arrangement in metallic glass contributes to many outstanding mechanical properties and good corrosion resistance, among others [3]. BMGs are characterized by the yield strength close to the theoretical values, large elastic strains (~2%), and the capacity for local plastic flow, which can result in extremely high fracture toughness of some glasses [4,5,6]. The superplastic-like viscous flow has been studied extensively near the glass transition to explore the potential for net shaping and forming. The combination of superior mechanical properties [7] and net shape formability [8,9] makes bulk metallic glasses promising new structural materials. Potential applications of metallic glasses include molding, printing, structural components, magnetic cores, coatings, damage-tolerant and bio-materials.

Experimental methods

The $Zr_{45+x}Cu_{45-x}Al_{10}$, (x=0,5,10,15,20) BMG samples were prepared by the arc-tilt casting method [10]. Master-alloy ingots were produced by arc melting mixtures of pure Zr, Cu, Pd, and Al metals in an argon atmosphere. In order to avoid oxygen contamination, a special high purity Zr (< 100 mass ppm oxygen) was used. The master alloy was completely re-melted and cast into a rod shape BMG (4 mm diameter × 60 mm height). The glass transition temperature and crystallization temperature were determined by calorimetric measurements (DSC) with a heating rate of 0.33 K/sec (20 deg/min). Thin slices of ~0.5 mm thickness were used for the X-ray diffraction experiments. High energy X-ray scattering experiments were performed at the beamline 6-ID. The incident energy was 100 keV, the beam size was 0.4 × 0.4 mm^2, and a 2 dimensional (2D) stationary detector was placed ~30 cm away from the sample. The 2D images were corrected for dark current and normalized to the incident beam monitor. The samples had comparable thickness, resulting in negligible systematic errors due to background and absorption corrections. Azimuthally integrated intensities were processed using the pdfgetX2 [11] package to obtain the structure function up to 24 $Å^{-1}$ and then the reduced pair distribution function G(r).

The reduced pair distribution function $G(r)$ is obtained by the direct Fourier-transformation of the total scattering function $S(Q)$, as given in Eq. 1, where $Q = 4\pi\sin(\theta)/\lambda$ is the modulus of the scattering vector, θ is the scattering angle and λ denotes the wavelength of the probe,

$$G(r) = 4\pi r(\rho(r) - \rho_0) = \frac{2}{\pi}\int_0^\infty Q[S(Q) - 1]\sin(Qr)dQ\,. \qquad (1)$$

The atomic pair density function $\rho(r)$ (PDF) can be obtained from G(r):

$$\rho(r) = \rho_0 + \frac{G(r)}{4\pi r}, \qquad (1a)$$

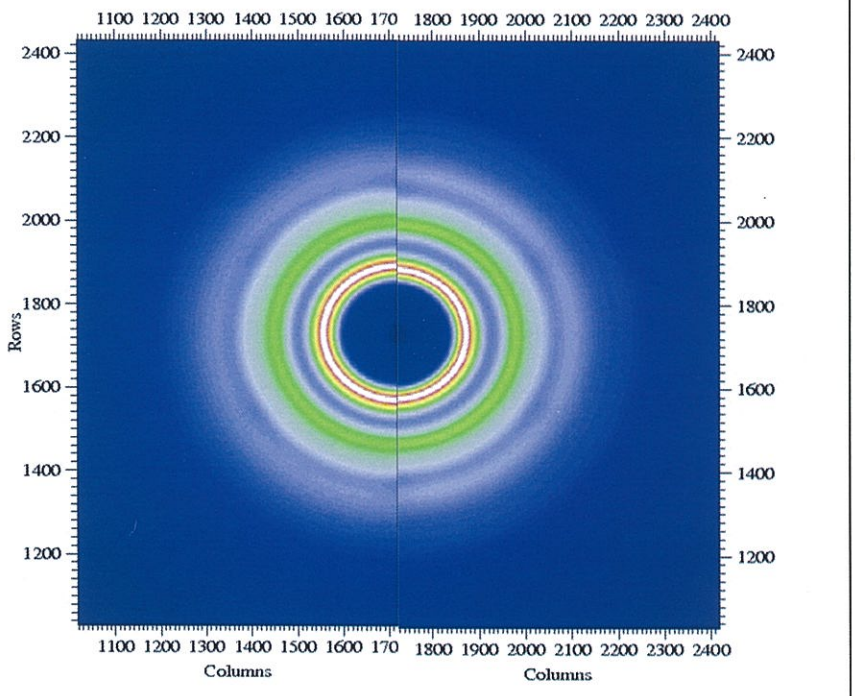

Figure 1. Halves of 2D diffraction patterns for Zr45 (left) and Zr65 (right) of ZrCuAl10 BMGs

where ρ_0 is the atomic density. The PDF is related to the pair distribution function $g(r)$, by $\rho(r) = g(r)\rho_0$ .The atomic PDF gives direct information about the distribution of the inter-atomic distances, albeit one dimensional due to spherical averaging.

Samples were measured in two orientations to assess the diffraction anisotropy from a 2D image. After the measurement was made in the first orientation, the sample was rotated by 90 degrees with respect to the original position, and the measurement was repeated. The difference between these two orientations should be zero for isotropic samples within errors due to monitor normalization and detector dark current correction. On the other hand, anisotropic patterns can be unambiguously detected [12]. This procedure confirmed the isotropic structure of BMG after tilt-casting.

The molecular dynamics (MD) simulations were performed using LAMMPS code using embedded atom potentials for Zr, Cu, and Al developed by Sheng et al. [13]. The standard npt setup included 32,000 atoms. The initial configuration was the f.c.c random alloy, which was melted at 2000 K. The 1000000 steps were carried out with resolution 1 fs. The atomic configuration was saved at every 50 ps. The temperature was varied by 50 degree to 300 K resulting in 10^{10} K/s cooling rate. The structure of cooled liquid and glass was resolved to obtain the partial pair distribution function. These were weighted by X-ray amplitudes to obtain compositionally averaged G(r) that could be compared with the experimental data.

Results and discussion

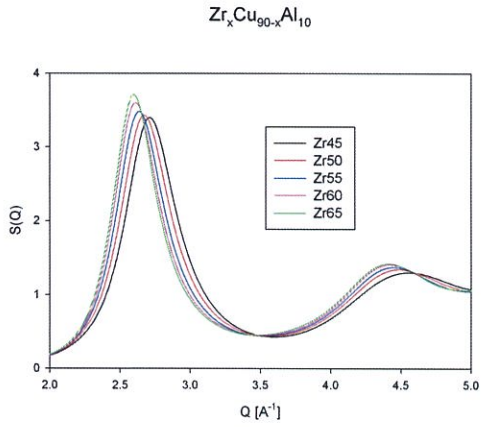

Figure 2. Strcuture function of the $ZrCuAl_{10}$ BMG alloys

The original 2D images for the two compositions of Zr=45 and 65 are shown in Figure 1. Both samples show diffuse scattering typical for metallic glasses. The different positions of the Debye rings reflect change in the structure as the compositio n is varied. This trend is clearly seen in the dependence of the structure function *S(Q)* on the relative Zr/Cu content as illustrated in Figure 2. With increasing Zr content, the peak high is increasing and is also shifted to the smaller Q values. This behavior is plotted in Figure 3. The top plot shows the dependence of the Q_p – the position of the peak of the *S(Q)*. The value of Q_p corresponds approximately to the average inter-atomic spacing in the structure: $\approx \frac{2.5\pi}{Q_p}$. The trend indicates that average inter-atomic spacing, d, (and atomic volume) is increasing with the increasing Zr content (inverse proportionality). This is consistent with the decreasing atomic density in this system. We may notice that the relation is linear between Zr=45 and Zr=60 at%. On the other hand the maximum at Q_p is quickly increasing with Zr content. The main peak height at the $S(Q_p)$ represents the efficiency of packing of the structural units in the structure and increasing packing order. For example, crystalline order would be reflected in dramatic increase in this peak height. This trend seems to be contradictory to the common perception of the order in the ZrCu based BMG glasses. It is believed that most important structural units in bulk metallic glasses are icosahedral clusters which tend to be Cu-centered. Addition of aluminum introduces some covalency into the system and improves this ordering – making icosahedra better geometrically defined. Thus, ordering should be better defined in Cu rich side. In fact, this is observed in the binary Zr-Cu glassy system. Therefore, the observed trend needs further investigation using alloys with higher Cu content.

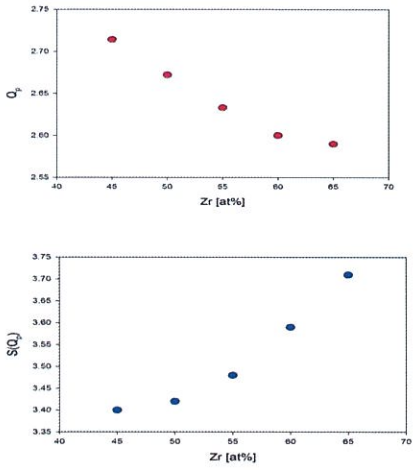

Figure 3. The composition dependence (Zr at%) of the $S(Q_p)$ and Q_p

Using the structure functions, *S(Q)*, shown in Figure 2, we obtained atomic pair distribution functions by performing isotropic Fourier transformation, using extended data up to 24 Å^{-1}. The results, *g(r)*, showing only first and second PDF peaks, are presented in Figure 4. The shape and position of the first peak is changing with the increasing Zr concentration. The first PDF peak is most heavily weighted by Zr-Zr and Zr-Cu contributions. The left-side shoulder corresponds to the average Cu-Zr distance and the right-side shoulder to the average Zr-Zr interatomic distance. With increasing Zr content we can observe that the right-side shoulder is increasing in height, reflecting an increase in the number of Zr-Zr pairs. At the same time, the whole peak is shifting to the right. This corresponds reasonably to the behavior of the Q_p in Figure 3 (plot at the top). Thus, the atomic volume is increasing with Zr content. We can also observe that change in the weighting of the Zr-Cu and Zr-Zr contribution is proportional to the Zr content up to 60 %at. Beyond 60 %at the change is rather small. The change in the shape of the broad peak in the PDF in the range between 4 and 6.6 Å is quite pronounced. It clearly indicates variation in the way the structure is organized in the medium range. The compatibility and packing of the structural motifs is changing in the glass with increasing Zr content.

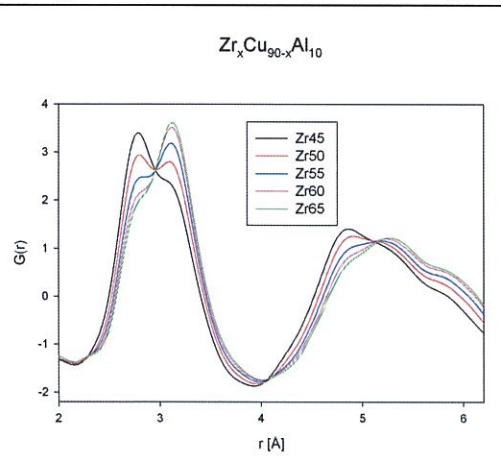

Figure 4. The PDF for the $(ZrCu)Al_{10}$ BMG alloys.

The experimental PDF for the three elements system is difficult to interpret directly. There are contributions from different chemical species, and also PDF is a spherical average projected on the radial distance. In such a case, molecular dynamic (MD) simulation may be helpful to understand compositional trends. The problem with MD is that it requires atomic potentials that have to be fitted to the alloy system. This is typically done using first principle calculations. Also, the cooling rate in MD is orders of magnitude higher than laboratory times. Therefore, MD results cannot be used literally, but rather to explain physical trends. We had performed MD calculation for the $Zr_{50}Cu_{40}Al_{10}$ alloy system. We used the resolved partial structure and

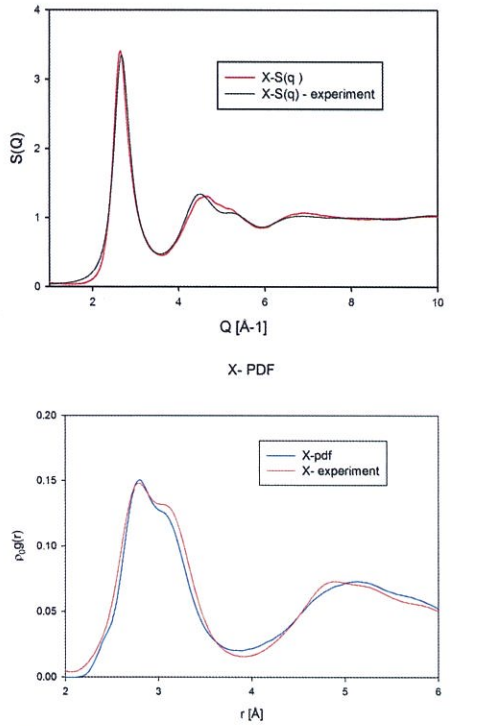

Figure 5. Comparison of the S(Q) and the PDF obtained by MD with experimental data.

pair correlation functions to obtain the total *S(Q)* and PDF that are weighted by the X-ray form factors. The results are shown in Figure 5. It is seen that experimental data are similar to the MD simulations; however, there are also distinct differences. The main difference is observed in the valley between first and second PDF peaks and shape of the second, broad PDF peak. The MD data represent more disordered structure, which is not surprising considering that it is obtained with such a high cooling rate. Therefore, the MD structure represents rather high temperature liquid. On the other hand, the first PDF peak is better defined in MD simulation, which indicates that MD is more sensitive to chemical ordering. Nevertheless, the MD data looks promising and we will continue to expand MD to other compositions to test the usability of the potentials and to find structural motifs that are changing with the Zr content in this alloy system. This project will be continued through additional diffraction experiments for Cu-rich alloys, MD simulations, and structural analysis.

I would like to thank sincerely Ms. Yuka Chiba for her help in "getting started" in Japan, and her constant, and firm supervision of administrative procedures and paper work.

Domo arigato gozaimasu!

[1] W.L. Johnson, MRS Bull, 24, (1999) 42–56.

[2] A. Inoue, Acta Mater., 48, (2000) 279–306.

[3] A. Inoue, T. Zhang and T. Masumoto, Mater. Trans. JIM, 31, 177 (1990).

[4] J.J. Lewandowski, W.H. Wang, A.L. Greer, Phil. Mag. Let., 85, (2005) 77–87.

[5] M.D. Demetriou, M.E. Launey, G. Garrett, J.P. Schramm, D.C. Hofmann, W.L. Johnson, R.O. Ritchie, Nature Materials, 10, (2011) 123–128.

[6] Q. He, J. K. Shang, E. Ma, J. Xu , Acta Materialia, 60, (2012) 4940–4949.

[7] A. L. Greer, Science, 267 (1995) 1947.

[8] J. Schroers, T.M. Hodges, G. Kumar, H. Raman, A.J. Barnes, Q. Pham, T.A. Waniuk, Mater. Today, 14, (2011) 14.

[9] J. Schroers, Phys. Today 66 (2), 32 (2013)

[10] Yokoyama Y, Inoue A, Fukaura K. Mater Trans 2002;43: 2316.

[11] Qiu X, Thompson JW, Billinge, SJL. J Appl Crystal 2004;37:678.

[12] Dmowski W, Egami T. J Mater Res 2007;22:412.

[13] Y.Q. Cheng, E. Ma, and H.W. Sheng, Phys. Rev. Lett, 102 (2009) 245501

各展示室見学・視察一覧

2013　7/30　日野自動車(株)常務役員他 4 名
9/30　戦略的基盤技術高度化支援事業第 3 回研究開発推進委員会出席者 9 名
11/13　セザス・ジャパン株式会社　2 名

新素材共同研究開発センターニュースvol.2
2013年11月30日

東北大学　金属材料研究所
附属新素材共同研究開発センター

〒980-8577　仙台市青葉区片平2-1-1
TEL 022-215-2371　／　FAX 022-215-2137
E-mail　crdam@imr.tohoku.ac.jp
URL　http://www.crdam.imr.tohoku.ac.jp